ResearchGate

See discussions, stats, and author profiles for this publication at: https://www.researchgate.net/publication/234916612

Origin of Nonlinear Recombination in Dye-Sensitized Solar Cells: Interplay between Charge Transport and Charge Transfer

ARTICLE *in* THE JOURNAL OF PHYSICAL CHEMISTRY C · NOVEMBER 2012

Impact Factor: 4.77 · DOI: 10.1021/jp3065179g

CITATIONS
20

READS
56

3 AUTHORS, INCLUDING:

José Pablo González Vázquez
Universidad Pablo de Olavide
8 PUBLICATIONS **139** CITATIONS
SEE PROFILE

Juan A Anta
Universidad Pablo de Olavide
109 PUBLICATIONS **1,799** CITATIONS
SEE PROFILE

Available from: Juan A Anta
Retrieved on: 27 January 2016

THE JOURNAL OF PHYSICAL CHEMISTRY C

Article

pubs.acs.org/JPCC

Origin of Nonlinear Recombination in Dye-Sensitized Solar Cells: Interplay between Charge Transport and Charge Transfer

J. P. Gonzalez-Vazquez,[†] Gerko Oskam,[‡] and Juan A. Anta*[,†]

[†]Área de Química Física, Universidad Pablo de Olavide, Sevilla, Spain

[‡]Departamento de Física Aplicada, CINVESTAV-IPN, Mérida, Yucatán, México

Supporting Information

ABSTRACT: Electron transfer between nanostructured semiconductor oxides and redox active electrolytes is a fundamental step in many processes of technological interest, such as photocatalysis and dye-sensitized solar cells. It has been shown that the transfer kinetics in the dye-sensitized solar cell are determined simultaneously by trap-limited transport and by the relative energetics of donor and acceptor states in the semiconductor and electrolyte. In this work, the transport and recombination mechanisms of photogenerated electrons in dye-sensitized solar cells are modeled by random walk numerical simulations with explicit description of the electron transfer process in terms of the Marcus−Gerischer model. The recombination rate is computed as a function of Fermi level in order to extract the electron lifetime and its influence on the electron diffusion length. The simulation method allows one to relate the recombination reaction order to the trap distribution parameter, the band edge position, and the reorganization energy. The results show that a model involving electron transfer from both shallow and deep traps, coupled with transport via shallow states, adequately reproduces all the experimental phenomena, including the dependence of the electron lifetime and the electron diffusion length on the open-circuit voltage when either the conduction band or the redox potential are displaced. Nonlinear recombination is predicted when the electron diffusion length increases with Fermi level, which is correlated with a reaction order different from one, in an open-circuit voltage decay "experiment". The results reported here are relevant to the understanding of the effect of using new electrolyte compositions and novel redox shuttles in dye-sensitized solar cells.

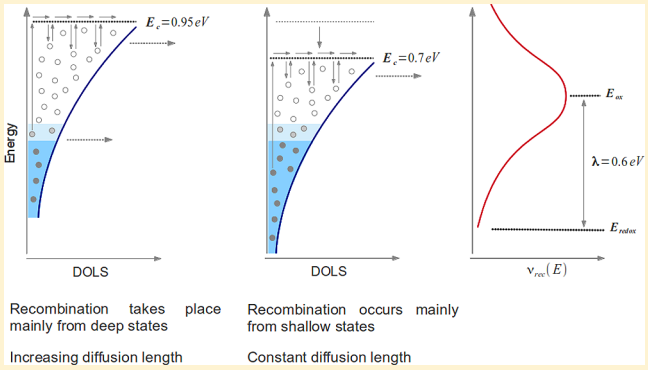

INTRODUCTION

Electron transfer across semiconductor oxide−electrolyte interfaces is a fundamental process in photocatalytic reactions[1−6] and in dye-sensitized solar cells (DSCs).[7−10] In nanostructured metal oxide electrodes, recombination between photogenerated electrons in the oxide and electron acceptors in the electrolyte at the semiconductor surface (dye cations) is a complex process in which the energetics of the semiconductor electronic structure and the distribution of relevant acceptor states play an important role. In addition, spatial disorder, such as the position of the reaction centers (recombination sites, traps, etc.), and charge transport in the nanostructured oxide and in the liquid electrolyte also influence the kinetics. Charge transfer reactions at the semiconductor−electrolyte interface also include electron injection.[11,12] The adequate description of these important charge transfer reactions is now becoming a primary topic in the theoretical description of nanostructured solar cells.

The fact that the recombination kinetics in the DSC exhibit nonlinear features was noticed more than 10 years ago in the work by Schlichthörl, van de Lagemaat, Frank, Peter, and their co-workers.[13−16] Recently, the importance of nonlinear recombination kinetics in DSC has again been stressed by Bisquert and Peter and their co-workers.[17−20] Nonlinear features are detected in the nonideal dependence of the open circuit photovoltage on illumination intensity (with a slope larger than 59 mV/decade) and in the nonideal behavior of the recombination resistance with respect to applied bias (measured via impedance spectroscopy[21−23]). Moreover, nonlinear effects result in the increase of the electron diffusion length as the electron density in the semiconductor is increased.[18−20,24]

Nonlinear recombination is normally expressed in terms of the kinetic equation

$$J_R = k_0 n_c^{\beta} \quad (1)$$

where J_R is the recombination current, k_0 is the kinetic constant, n_c is the density of free (conduction band) electrons, and β is the reaction order. A reaction order of one, indicative of simple unimolecular recombination via conduction-band states, leads

Received: July 2, 2012
Revised: September 24, 2012
Published: October 2, 2012

ACS Publications © 2012 American Chemical Society

dx.doi.org/10.1021/jp306517g | J. Phys. Chem. C 2012, 116, 22687−22697

to an ideal slope of 26 mV (59 mV/decade) in the open-circuit voltage (V_{oc})−log(illumination intensity) plot[25] and to an electron diffusion length that is constant with respect to illumination intensity. However, reaction orders ranging between 0.6 and 0.8, indicative of *sublinear* recombination kinetics with respect to free electron density, are generally found in dye-sensitized solar cells.[20,23,26−29] The reaction order has important implications for the photoconversion efficiency. Assuming an ideal dependence of the free electron density with respect to voltage, eq 1 leads to a current−voltage curve given by[18]

$$J = J_{sc} - J_0[\exp(\beta eV/k_B T) - 1] \quad (2)$$

where e is the elementary charge, V the applied bias (or photovoltage), k_B the Boltzmann constant, and T the absolute temperature, and J_{sc}, J_0, and J are the short-circuit photocurrent, the exchange-current, and total photocurrent densities, respectively. Equation 2 predicts that reaction orders significantly smaller than one lead to current−voltage curves with small fill factors, hence showing a reduced efficiency with respect to an "ideal diode" solar cell. The recombination losses can be enhanced under illumination, as recently discussed.[30,31]

The goal of this work is to understand the effect that the energetics of the redox pair and semiconductor produce on the transport−recombination kinetics. In addition, we pursue to determine the fundamental origin of a reaction order different from one. To do so, we analyze the recombination kinetics at the semiconductor oxide−electrolyte interface starting from the molecular mechanisms involved in the electron transfer reaction. As it is generally accepted that electron trapping plays a significant role in the recombination reaction,[17,32,33] we focus here on the interplay between the energetics of the electrons in the semiconductor nanostructure and the density of states of the electron acceptors. Hence, we combine the theoretical description of trap density distributions[34,35] and trap-limited transport[24,36−38] with the well-known Marcus−Gerischer (MG)[25,39] theory of charge transfer at semiconductor−electrolyte interfaces.

It is important to review previous work relevant in this topic. The MG model has been utilized by Bisquert and coworkers[23,40] to describe the kinetics or recombination from a distribution of localized states to a distribution of acceptor states in the electrolyte. In summary, their approach is based on the equation

$$J_R = ed\int_{E_{redox}}^{E_c} g(E)f(E - E_F)P_R(E)dE \quad (3)$$

where e is the elementary charge, d is the film thickness, $g(E)$ is the density of localized (donor) states, $f(E - E_F)$ is the occupation probability at a certain position of the electron quasi-Fermi level E_F, and $P_R(E)$ the probability of recombination at a given value of the energy (density of acceptor states). Equation 3 simply states that the recombination rate is a consequence of the interplay of three contributions: the number of states available at each value of the energy in the semiconductor (described typically by an exponential distribution), the probability that this energy state is occupied (Fermi−Dirac), and the probability of charge transfer to the electrolyte (which includes the number of states available), as determined by the MG formula. To obtain the net recombination rate, the product of these three probabilities should be integrated over all to all values of the energy between the redox Fermi level (E_{redox}) and the semiconductor conduction band edge (E_c). Starting from this basic scenario, Bisquert derived an approximate analytical expression for the recombination rate[23,40] applying the zero temperature limit of the Fermi−Dirac distribution and assuming that the Marcus reorganization energy is much larger than the photovoltage. According to this simplified formalism, the reaction order is

$$\beta = 1/2 + T/T_0 \quad (4)$$

where T_0 is the characteristic temperature of the exponential distribution of localized states. Hence, for characteristic temperatures or around 900−1200 K,[35,41] reaction orders of ∼0.75−0.85 are predicted, close to the experimental values. This model is also successful in predicting the correct temperature dependence of the reaction order,[17] although abnormally high characteristic temperatures seem to be required to fit the experimental data. On the other hand, to assume that the reorganization energy is much larger than the photovoltage may be too strong of an approximation, since reorganization energies on the order of 0.4−1.2 eV are commonly reported for typically used redox couples.[33,39,42−44] An additional complication is that assuming that the reorganization energy is very large excludes the possibility that the system may enter the Marcus inverted regime, a situation that has been claimed in the literature.[20,39]

MG theory has recently also been applied by Ondersma and Hamann[44] to successfully predict the shape of the electron lifetime curve versus voltage in DSCs with outer-sphere redox shuttles. The formalism of these authors is also based on the description represented by eq 3, but with explicit consideration of inner and outer sphere reorganization energies in the calculation of $P_R(E)$. The model devised by these authors includes electron transfer mediated by surface states that can play a significant role in the recombination reaction. More recently Ansari-Rad et al.[45] also used eq 3 as a starting point to devise a theoretical model where the β exponent is calculated as a function of the Fermi level, showing that it is always less than unity, except when the Fermi level approaches the conduction band. It has to be noted that most of these previous studies focused on the determination and analysis of the electron lifetime, a magnitude which is usually measured at open-circuit or at a flat Fermi level. However, a solar cell under working conditions does not operate at open circuit, but in the presence of a density gradient, which drives electrons to the external contact. Hence, the interplay between transport and recombination (as manifested by the value of the diffusion length) is decisive for good electron collection under real operating conditions.

In a previous paper,[24] we applied the random-walk numerical simulation method (RWNS)[36−38] to evaluate the lifetime (τ_n) and the diffusion length (L_n) for electrons moving in an exponential distribution of trap energies. This procedure requires one to incorporate recombination kinetics in the algorithm, which was assumed to occur according to a constant probability. This way, only trapping/detrapping events and the population of the electronic states (traps) contribute to the Fermi level dependence of τ_n and L_n. Using this simplified method, the compensation effect predicted by various authors[46−49] can be nicely reproduced from a microscopic mechanism of transport/recombination. In another paper[50] we showed how the effect of the morphology of the photoanode on electron collection can be suppressed if the recombination kinetics are too rapid or too slow. In this paper we extend this work by introducing a nonconstant recombination probability,

which depends on the energy of the donor and the acceptor state according to the MG model.[25,51] As stated in eq 3, the probability of recombination and the recombination rate should depend on the population of electronic states in the semiconductor (controlled by the Fermi level position) and the reorganization energy of the redox couple in the electrolyte. It is expected that all these microscopic parameters produce complex kinetics that cannot be described by a reaction order of one.

The aim of this work is 2-fold: on the one hand, we intend to analyze the problem posed by eqs 1−3 from first principles, using RWNS as a versatile tool to study, *simultaneously*, transport and recombination. On the other hand, we intend to extend previous theoretical work by establishing unambiguously the effect of the reorganization energy and the relative positions of redox energy and conduction band on both the diffusion length and the lifetime.

METHODOLOGY: RANDOM WALK NUMERICAL SIMULATION WITH RECOMBINATION VIA ELECTRON TRANSFER TO THE ELECTROLYTE SOLUTION

The RWNS method[36−38] is a stochastic calculation that makes it possible to obtain dynamic properties in disordered media starting from basic assumptions about the transport and recombination mechanism. In a RW simulation a number of carriers is allowed to move at random in a three-dimensional network of sites. According to the selected transport model, each site in the network is given a certain release or detrapping time that determines the jumping rate or probability for a carrier to jump to another site. If we consider a multiple-trapping (MT)[52] mechanism of charge transport and no external electrical fields, the detrapping time depends only on the energy of the starting site E_i according to the expression[36,53]

$$t_i = -\ln(R)t_0 \exp[(E_c - E_i)/k_BT] \quad (5)$$

where R is a random number uniformly distributed between 0 and 1 and E_c is the energy of the extended state through which transport is assumed to occur, i.e., the mobility or conduction band edge. In eq 5 t_0 is an adjustable parameter that controls the time scale of the simulation. This is usually defined in terms of attempt-to-jump frequency ($\nu_0 = 1/t_0$), characteristic of the material.

In this work we run the random walk simulation on a three-dimensional network of traps distributed randomly and homogeneously in space. The energies of the sites are taken from an exponential distribution[35]

$$g(E) = \frac{N_L}{k_BT_0} \exp[(E - E_c)/k_BT_0] \quad (6)$$

where N_L is the total trap density, and T_0 is the characteristic temperature of the distribution.

Details on the organization of a RW simulation based on times are given in previous reports[24,38,53,54] and in the Supporting Information, where "frequently asked" questions about the method are answered. In summary, the numerical algorithm proceeds as follows: electrons are placed initially at random, and after generation of random numbers "R", they are given release times according to eq 5 and the energies of the sites they occupy. Waiting times are defined as the difference between the release time of the carrier and the time already spent by the carrier in a particular site. For each simulation step the carrier with the shortest waiting time (t_{min}) is allowed to move. The waiting times for the rest of the carriers are then reduced by t_{min}, and the process is repeated such that the simulation advances by time steps of length t_{min}. This *time-adaptive* simulation permits one to efficiently sample systems characterized by a very large dispersion of site energies such as those derived from eq 6, which produces a very large dispersion of detrapping times.

In this work, we have introduced an energy-dependent recombination mechanism in the RWNS algorithm, which is described by the MG model. The MG model has been introduced previously by a number of authors[17,25,39,40,44,45] to describe recombination in DSCs. To our knowledge, this paper represents the first time that MG theory is incorporated in a RWNS calculation. Basically, this is done by giving a *recombining character* to the network of traps in such a way that its energy distribution serves as the medium from which a direct charge-transfer from traps is applied. However, in order to achieve a complete recombination model, two alternative stochastic procedures based on the MG description have been implemented. It has to be noted that these two models represent different recombination mechanisms, in which transport plays a distinct role.

The first recombination procedure brings about the computation of a probability of recombination each time an electron reaches a trap of energy E. This is obtained via the following expression

$$P_R(E) = k_{r0}\sqrt{\frac{k_BT}{4\pi\lambda}} \exp\left(\frac{-(E - E_{ox})^2}{4\lambda k_BT}\right) \quad (7)$$

with $k_{r0} = 2k_{tr}c_{ox}$, where k_{tr} is a time constant for tunneling, c_{ox} is the concentration of oxidized species in the electrolyte, λ is the reorganization energy, and E_{ox} is the most probable oxidation energy level. Note that P_R is a dimensionless quantity. This description, which we will call model 1, can be seen as an extension of our previous work in which a constant recombination probability is replaced by a more realistic energy-dependent probability.[24] By this procedure we can simulate the interplay between the random walk of the electrons and the charge transfer to the electrolyte.

The second recombination procedure involves a formulation based on times instead of probabilities. Thus, the waiting times numerical algorithm is modified in such a way that each electron is assigned a recombination time along with its detrapping time. These recombination times are computed according to the inverse of eq 7

$$t_i^{rec} = -\ln(R)t_{r0}\sqrt{\frac{4\pi\lambda}{k_BT}} \exp\left(\frac{(E_i - E_{ox})^2}{4\lambda k_BT}\right) \quad (8)$$

where R is a random number uniformly distributed between 0 and 1 and t_{r0} is a adjustable prefactor that controls the time scale of recombination. The implementation of this algorithm (that we will call model 2) is as follows: once charge carriers have been injected, detrapping and recombination times are computed for all of them via eqs 5 and 8, respectively. Both types of times are stored in the same list of waiting times in such a way that if the minimum time corresponds to detrapping, that carrier is selected to move into its target site. On the contrary, if the minimum time corresponds to recombination, the carrier is removed from the sample. Once either the move or the recombination is executed, both

detrapping and recombination times of the rest of the carriers are reduced by t_{min}.

A mechanism based on times rather than on rates or probabilities leads, in principle, to the same results because according to eqs 7 and 8 a low recombination time is equivalent to a high recombination rate (and vice versa). However, there is an important difference between both models, which is based on the sequence in which the moves are executed in the simulation. In model 1 the MG formula is applied *after* each detrapping event. Hence, transport will influence recombination to some extent. On the contrary, in model 2, the application of the MG formula runs in *parallel*. Hence, transport and recombination are separated or uncorrelated. Furthermore, in model 2 *direct transfer* between trapped electrons and electrolyte acceptors is possible, whereas in model 1, only electrons that have been previously detrapped (i.e., *quasifree* electrons) are allowed to recombine. In both models, however, recombination can take place starting from any trap state (either via a previous detrapping or by direct transfer) and not only from the conduction band.[47] This is a reasonable assumption if we consider that the great majority of electrons will be trapped (approximately 90% as recently estimated)[33] and that electrons spend a much longer time in trapped states than in the conduction band.

It must be noted that in the RWNS formalism utilized here there is strictly *no conduction band* level. E_c is just the parameter that determines the transport activation energy in the multiple-trapping description of eq 5 and the origin of energies in the exponential distribution of eq 6. Furthermore, simulation times are always normalized with respect to t_0 in eq 5, which represents the average residence time of electrons in the conduction band. Hence, electrons do no effectively *stay* in the conduction band and they cannot undergo direct recombination from the conduction band, *within* this particular formalism. However, as the mechanism of recombination based on eq 7 (model 1) involves that electrons should get detrapped before they have the possibility to undergo a recombination event, it can be seen as an alternative view to a "conduction band recombination probability" under certain conditions. In fact, if we bear in mind that detrapping times from shallow traps are much shorter than from deep traps and that most of the sites have energies close to the "conduction band", one expects that model 1 samples preferentially recombination from shallow traps whereas model 2 samples recombination from deep traps.[55]

In this work, we study the Fermi level dependence of the electron diffusion length for both kinds of recombination mechanisms. In addition, we present the results for a hybrid model, which is a combination of both. In all cases, the recombination rate of specific electrons will depend on their energies and this will introduce a number of *recombination events* in the simulation for a given set of input parameters. Hence, the objective of the simulation procedure is to store the time and the distance that electrons survive/travel before they recombine. As we will see below, only the hybrid model is capable of adequately reproducing the behavior of the system with respect to Fermi level and conduction band position. In Figure 1, a schematic representation of the numerical procedure and the physical processes involved is shown. Using the different models, we perform random walk simulations of two experiments that are generally used to characterize recombination kinetics: (i) determination of kinetic parameters under constant illumination intensity and under open circuit voltage conditions and (ii) open circuit voltage decay measurements upon switching off the light source.

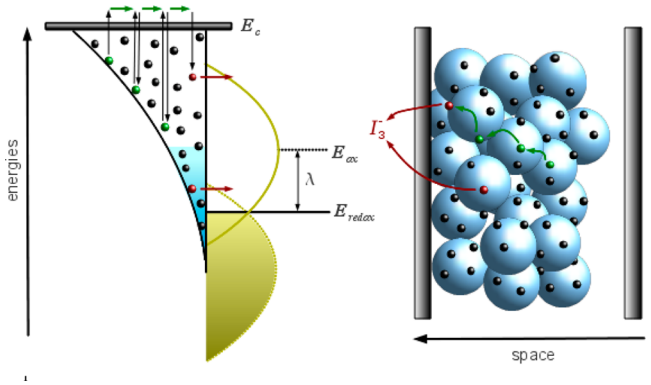

Figure 1. Illustration of the transport and recombination processes studied in this work. The meaning of the reorganization energy (λ) and the Fermi level position (showed as a shaded region) are indicated in the figure.

In a first kind of simulation (steady-state RWNS), as the solar cell is simulated at open-circuit conditions and under constant illumination intensity (fixed Fermi level), a constant electron density should be maintained in the sample. This is achieved by imposing the restriction that when an electron has just recombined, another electron is immediately injected into the system in another place at random. For this *fresh* electron, both time and distance are reset such that the average time and distance between recombination events can be computed, stored, and represented versus total simulation time. Finally, these magnitudes are renormalized by the total number of electrons and the total number of recombination events so that the result is effectively an average time and distance for one single electron. We have previously demonstrated that this procedure yields *true* electron lifetimes and diffusion lengths.[24]

In a second kind of simulation (transient RWNS), the restriction of reintroducing electrons is removed. This procedure makes it possible to simulate a typical open-circuit voltage decay experiment.[51] As no new electrons are introduced after recombination, the concentration of electrons in the sample decreases with time according to certain kinetics. It has been found that this decay can be described by a power law, such that the reaction order β with respect to free electron density can be extracted by means of a fitting procedure to the integrated version of eq 1.

The electron lifetime is defined in its more general form by[17,56]

$$\tau_n = \left(\frac{\delta U_n}{\delta n}\right)_n^{-1} \tag{9}$$

where U_n is the recombination rate (J_R/e) and n is the total electron density. The lifetime is hence defined as the variation of the recombination rate for small variations of the total density, and it is the lifetime extracted from small-perturbation techniques such as impedance spectroscopy. Alternatively, a pseudo-first-order lifetime can be defined[30,45,57,58]

$$\tau_1 = -\frac{n}{\mathrm{d}n/\mathrm{d}t} \tag{10}$$

As shown in ref 45, both lifetimes are not equal. In ref 58 it has been shown that both are proportional to each other and related by a constant (equal to α/β).

dx.doi.org/10.1021/jp306517g | J. Phys. Chem. C 2012, 116, 22687−22697

In this work, we use eq 10 to extract the lifetime from the transient RWNS calculations. It is shown that this procedure reproduces the values of lifetimes obtained from the "average" method described above, for the same Fermi level, quite accurately. This is consistent with our findings in ref 24, where it was found that the distribution of survival times for electrons was exponential in a simulation performed at constant Fermi level, corresponding to first-order recombination kinetics. The time constant of this distribution coincided with the lifetime obtained by averaging the survival times of the electrons.

In order to keep the number of adjustable parameters as small as possible, we have employed values reported in the literature for most of the parameters used in the simulations.[24,39] Hence, we use T_0 = 700−1100 K, T = 300 K, N_L = 10^{27} m^{-3} (meaning an average trap−trap distance of 1 nm), and t_0 = 10^{-14} s. A cutoff radius of 1.5 nm is introduced in the simulation so that jumps to neighbored traps beyond this distance are not considered. To study the effect of a shift of the band edges, we have used two different values for the position of the conduction band extracted from the work of Jennings and Wang:[39] E_c = 0.95 eV for the case of no additives and E_c = 0.7 eV in the presence of 2 M Li^+. The only adjustable parameters are those controlling recombination [k_{r0} or t_{r0} (or both) and λ]. Independent adjustment of k_{r0} and t_{r0} gives us freedom to prioritize one model over another. Both parameters depend on the distance between electron and acceptors and can vary with the composition of the electrolyte. For instance, addition of adsorptive especies such us TBP or Li^+ can increase the distance between electrons in the semiconductor and the redox-active ions, as suggested by Nakade et al.[43] Furthermore, different tunneling factors are expected for traps of different energy. For simplicity, we have considered both k_{r0} and t_{r0} factors independent of energy.

As we will see below, the adjustment of k_{r0} and t_{r0} for each model (and the ratio of them in the case of a combination of both) does not modify the Fermi level dependence of the lifetime and the diffusion length, so we are able to represent the results normalized by the maximum value of the measured magnitudes in each case (see Supporting Information for details). Moreover, to avoid excessive computational times, systems with relatively small diffusion lengths have been simulated with the restriction that it must always be ensured that the time scale for trapping/detrapping is much shorter than the time scale of recombination, as shown in our previous work.[24] Finally, a sufficient number of independent simulations (defined for different random number sequences) have been carried out in order to ensure good statistics in the final results.

RESULTS AND DISCUSSION

Results of steady-state RWNS simulations using model 1 for two different values of the reorganization energy are presented in Figure 2 (upper panel). The electron diffusion length is shown as a function of the energy difference $E_F - E_{redox}$, which corresponds to the open-circuit voltage (V_{oc}) produced by the solar cell at steady-state. In the dark, $E_F - E_{redox}$ = 0, and the system remains in thermodynamic equilibrium.

It is observed that the diffusion length increases with V_{oc} with an energy-dependent recombination probability provided that the reorganization energy is sufficiently low (i.e., λ = 0.2 eV). In contrast, for a higher reorganization energy (λ = 0.6 eV), the electron diffusion remains constant. The predictions of model 1 presented in Figure 2 can be explained as follows. For an exponentially increasing trap density distribution, the detrapping probability of electrons increases upon shifting the Fermi level to higher energies. This makes transport more rapid, as shown, for instance, in ref 24. However, the probability of recombination also depends on the number of acceptor states, as described by eq 7. At this point, two scenarios can be observed: (1) *linear regime*, where, for a redox couple with a reorganization energy larger than V_{oc}, the recombination probability is increased due to the increase of the density of available acceptor states upon raising the Fermi energy, resulting in a compensation effect that keeps the diffusion length approximately constant, and (2) *nonlinear regime*, where, for redox couples with a small reorganization energy, the recombination probability decreases with increasing V_{oc} when the system enters the Marcus inverted region. In this case, the diffusion length is expected to increase with increasing (open-circuit) voltage, since the recombination kinetics become slower due to the lower probability of electron transfer to the solution.

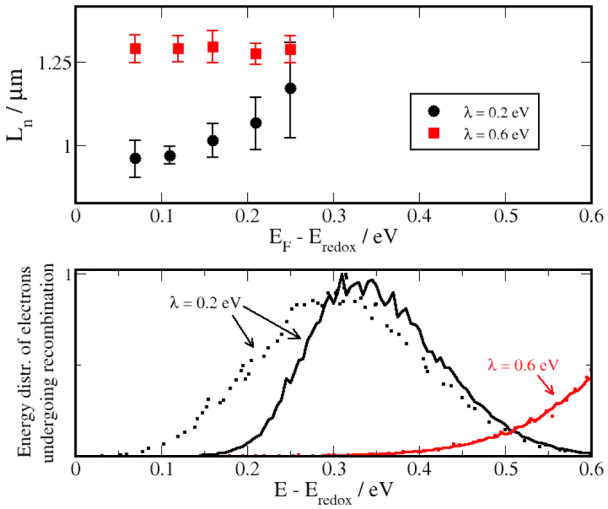

Figure 2. (Top) Electron diffusion length calculated by steady-state RWNS calculations using model 1 for two values of the reorganization energy. Bottom: Distribution of trap energies from which electrons undergo a recombination event. The same two values of the Fermi level are shown for both reorganization energies: $E_F - E_{redox}$ = 0.25 eV (black and red dashed lines) and $E_F - E_{redox}$ = 0.07 eV (balck and red dashed lines). The characteristic temperature of the trap energy distribution utilized in the simulation was T_0 = 1100 K and a band offset of $E_c - E_{redox}$ = 0.7 eV was considered. The following parameters have been used for recombination: k_{r0} = 3 × 10^{-4} arbitrary units (arb units) for λ = 0.2 eV and 8 × 10^{-6} arb units for λ = 0.6 eV. See eq 7 and text for details. Note that simulations are stopped at $E_F - E_{redox}$ = 0.25 eV, once the trend of the diffusion length is well-established, to avoid excessive computational times.

The origin of the dissimilar behavior of the diffusion length can also be understood by inspecting the lower panel of Figure 2, where the distribution of trap energies from which the electrons undergo a recombination event is shown. For the case in which the diffusion length does not increase with voltage, this distribution is exponential, indicating that most electrons recombine from states close to the conduction band. On the other hand, when the diffusion length increases with voltage, the distribution exhibits a maximum at intermediate energies. The appearance of this maximum is a consequence of the interplay between two opposite effects: the increase of the density of donor states characteristic of an exponential function and the decrease of the density of acceptor states as the energy

dx.doi.org/10.1021/jp306517g | J. Phys. Chem. C 2012, 116, 22687−22697

of the electron is raised. More importantly, the two regimes differ in another feature. For the linear case the distribution of states from which recombination occurs does not change when the Fermi energy, i.e., the electron density, is varied. Hence, the diffusion length remains constant. On the contrary, for the nonlinear case the distribution maximum gets displaced toward lower energies. This change in the recombination probabilities explains why the diffusion length tends to increase as more electrons are accumulated in the semiconductor for the nonlinear case.

The previous result shows that a nonconstant behavior of the diffusion length with respect to V_{oc} (nonlinear regime) can be reproduced with an energy-dependent recombination probability using model 1. However, it must be recognized that this regime is only accessible if the open-circuit voltage is above the most probable oxidation energy in the electrolyte (E_{ox}), i.e., in the Marcus inverted regime. This last requirement implies that for typical values of the open circuit voltage of standard DSC of 0.6−0.8 V, very small values of the reorganization energy are needed. However, values below λ = 0.4 eV are rather unrealistic.[44] On the other hand, the models of Bisquert et al.[17,25] and Villanueva-Cab et al.[59] show consistent formalisms according to which an increasing electron diffusion length with respect to V_{oc} can be achieved by assuming much higher values of the reorganization energy. Hence, it is concluded that model 1 does not achieve an adequate description of nonlinear recombination in DSCs, implying that other charge-transfer mechanisms must be taking place.

As described in the previous section, the alternative model 2 assumes that direct transfer between trapped electrons and electron acceptors can take place. This is implemented by computing recombination times via eq 8 and allowing for removal of electrons when these times are shorter than the transport times, in accordance with the usual RWNS algorithm. Steady-state results for the electron diffusion length obtained by model 2 are presented in Figure 3.

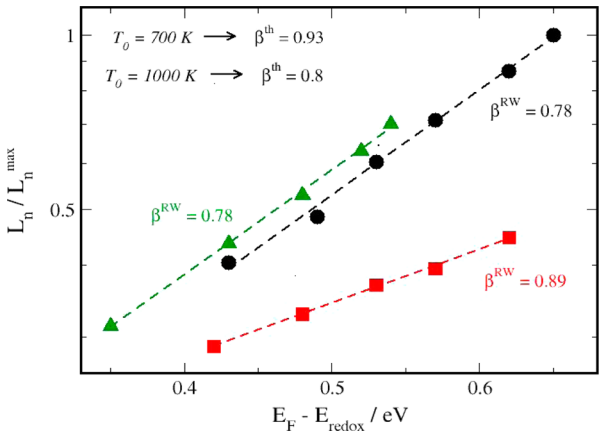

Figure 3. Electron diffusion length calculated by steady-state RWNS calculations using model 2 for different values of the reorganization energy and characteristic temperature: T_0 = 700 K and λ = 2 eV (circles), T_0 = 700 K and λ = 20 eV (squares), and T_0 = 1000 K and λ = 20 eV (triangles). Results are obtained from the Marcus−Gerischer formula (eq 8) and a density of electronic states in the semiconductor given by eq 6. A band offset of $E_c - E_{redox}$ = 0.95 eV was considered. Dashed lines correspond to fits to eq 11. "Theoretical (th)" and "simulated (RW)" values of the adimensional parameter β are also indicated in the graph.

First of all, it can be observed that, in contrast to model 1, model 2 predicts an increasing diffusion length versus the open-circuit voltage for a high value of the reorganization energy. Moreover, the curves exhibit exponential behavior in accordance with previous theoretical models[17,59] where the following theoretical formula is derived[17]

$$L_n = B \exp\left[\frac{(1-\beta)}{2k_B T}(E_F - E_{redox})\right] \quad (11)$$

with a theoretical value for the exponential parameter given by (same as eq 4)

$$\beta = 1/2 + T/T_0 \quad (12)$$

Although simulations with model 2 do indeed predict an exponential behavior, the parameter β extracted by fitting to eq 11 does not coincide with the theoretical value of eq 12. This is due to the fact that eqs 11 and 12 are derived under the assumption that the reorganization energy is several orders of magnitude larger than the open-circuit voltage (which is indeed a strong approximation). As a matter of fact, curves in Figure 3 using a reorganization energy of λ = 20 eV do offer a possibility to test the prediction of eq 12. Such an unrealistic value of the reorganization energy (although otherwise appropriate for theoretical reasons) permits us to obtain simulated slopes closer to the theoretical values of eq 12. On the other hand, model 2 reproduces qualitatively the temperature dependence of the diffusion length. Thus, it is found that for T_0 = 1000 K the slope of the $\log(L_n/L_n^{max})$ vs $(E_F - E_{redox})$ curves is higher than for T_0 = 700 K, in accordance with the theoretical prediction of eq 12.[17] In summary, model 2 seems adequate to explain many of the experimental facts as well as the occurrence of a nonlinear regime.

However, it is essential to find a model that it is capable of reproducing *all* experimental observations in DSCs in order to clarify the charge-transfer mechanisms involved in this type of solar cells. In this context, recent reports by Jennings et al.[20,39] showed that it is possible to induce a change from the nonlinear to the linear regime by addition of lithium ions to a iodide/triiodide electrolyte. This change has been interpreted as a consequence of the displacement of the semiconductor conduction band toward more positive potentials upon Li^+ addition. To describe this observation, we have carried out simulations for different values of the E_c parameter with respect to the electrolyte equilibrium redox level, but keeping the total number of traps constant. In this context it has to be noted that some authors[33,44,60] have pointed out that the electrochemistry of the iodide/triiodide system is very complicated, as it involves a multielectron process and intermediate species such as I_2^-. However, in this work we do not study the actual mechanism of electron transfer but the effect that the relative positions of conduction band and redox level, as well as the reorganization energy, have on the recombination kinetics. Even if charge transfer is produced to I_2^- instead of I_3^-, there will always be a distribution of acceptor energies given by eq 7, which would be sensitive to displacement of either the conduction band in the semiconductor or the equilibrium redox level of the electrolyte.

Results for both models 1 and 2, together with experimental results from refs 20 and 39 for two compositions of the electrolyte, can be found in Figure 4. As indicated in the previous section, we can represent results normalized with respect to the maximum value for both experimental and simulated cases. The simulation results show that it is possible

dx.doi.org/10.1021/jp306517g | J. Phys. Chem. C 2012, 116, 22687−22697

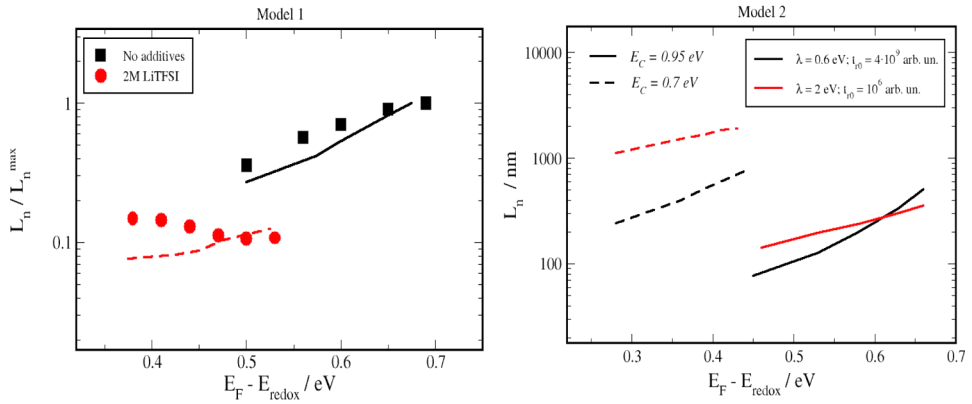

Figure 4. (Left) experimental measurements (ref 20) of the electron diffusion length for a DSC with Li^+ (red circles) and without Li^+ ions (black squares) in the electrolyte, and the predictions of model 1 with λ = 0.25 eV, T_0 = 700 K, and T = 300 K are presented. Values of $E_c - E_{redox}$ = 0.7 eV (red dashed line) and 0.95 eV (black solid line) are used for a DSC with and without Li^+ ions in the electrolyte, respectively. Different values of k_{r0} (see eq 7 have been used for each case: $k_{r0} = 5 \times 10^{-5}$ arb units for $E_c - E_{redox}$ = 0.7 eV and 5×10^{-4} arb units for 0.95 eV. (Right) Predictions of model 2 with the same parameters: T_0 = 700 K, T = 300 K, $E_c - E_{redox}$ = 0.95 eV (solid lines) to 0.70 eV (dashed lines). Two values of the reorganization energy: λ = 2 eV (red) and λ = 0.6 eV (black) are shown for each type of electrolyte.

to approximately reproduce the experimental curves using model 1. However, again, an unrealistic low value for the reorganization energy (λ = 0.25 eV) is required. On the other hand, it is observed that, if we use model 2, the diffusion length slope cannot be changed when the band is displaced, neither by using a large reorganization energy (λ = 2 eV) nor an intermediate one (λ = 0.6 eV).

The change of the electron diffusion length behavior upon band displacements has been interpreted as a modification of the main recombination mechanism involved in the semiconductor/electrolyte interface, from recombination via trap states to recombination via conduction band states.[20,39] Here it is important to stress again that model 1 can be interpreted as an alternative view of the so-called conduction band recombination if a high enough reorganization energy is applied. Indeed, it can be seen in Figure 2 that, when the reorganization energy is higher than the photovoltage, the energy distribution for electrons undergoing recombination is exponential, meaning that most of the sites from which recombination events occur are those very close to the conduction band edge. These shallow states correspond to "nearly free" electrons, which are more likely to recombine. Hence, for an exponential distribution of trap energies, the shallow states (close to E_c) play the role of an *effective* conduction band, with faster transport and more rapid recombination if there are acceptor states available close to $E = E_c$. At the same time, model 2 has proven to be ideal to reproduce recombination from deep traps due to its capacity to reproduce theoretical features that take into account this specific charge-transfer mechanism. In summary, it is reasonable to assume that an adequate combination of the two models may be able to explain all the experimental phenomenology, including the effect of the change of the diffusion length slope when plotted versus V_{oc}.

In the following, RW simulation data as obtained by a combination of models 1 and 2 (hybrid model) are presented. In these simulations, electrons being detrapped are allowed to recombine by generating probabilities with eq 7, as defined by model 1. Simultaneously, immobile electrons are also allowed to recombine directly from traps according to waiting times obtained by eq 8, as defined by model 2. The relative weight of each type of recombination is controlled by adjusting the parameters k_{r0} and t_{r0}, respectively.

Results obtained by this hybrid model, along with experimental data for different compositions of the electrolyte, are shown in Figure 5. The calculations were carried out using

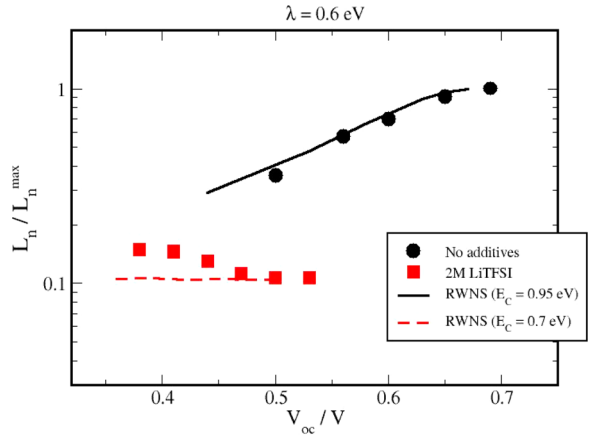

Figure 5. Electron diffusion length from experiments (symbols) and calculated by steady-state RWNS calculations (lines) using the combination of model 1 (eq 7) and model 2 (eq 8) (hybrid model). The simulations correspond to a system defined by λ = 0.6 eV, T_0 = 700 K, T = 300 K, and $E_c - E_{redox}$ = 0.95 (black) and 0.7 eV (red), using $k_{r0} = 8 \times 10^{-5}$ arb units and $t_{r0} = (1.25 \times 10^8)t_0$. Note that data are normalized with respect to the maximum value.

T_0 = 700 K, T = 300 K, λ = 0.6 eV, $k_{r0} = 8 \times 10^{-5}$ arb units, $t_{r0} = (1.25 \times 10^8)t_0$. The simulation results show that it is possible to reproduce the change of slope observed experimentally for realistic values of these microscopic parameters. It is observed, however, that a displacement of the conduction band toward lower energies (more positive electrochemical potentials), leads to longer diffusion lengths (shown in Supporting Information, Figure S1). Larger values of the electron diffusion length have been found experimentally when lithium ions are added in the electrolyte.[39] However, it has been reported[20] that freshly fabricated DSCs with LiTFSI (simulated system) exhibited higher L_n than DSC with no additives and that after a certain time L_n decreased, although the dependence with respect to the

dx.doi.org/10.1021/jp306517g | J. Phys. Chem. C 2012, 116, 22687−22697

open-circuit voltage is preserved. The lowering of the electron diffusion length while the dependence was maintained has also been reproduced, as can be seen in Figure 5. To achieve this we have modified the prefactor k_{r0} in eq 7, specifically from 8×10^{-5} to 2.5×10^{-3} arb. units. It has to be noted that in ref 20 results for a stable cell based on LiI have also been reported. However, in this work we have focused on the LiTFSI, as we aimed to study the energetics at the same voltage range.

One might argue that the chosen value of the reorganization energy is somehow arbitrary. Hence, we have tried to fit the experimental data using a larger value of the reorganization energy. Results of these RW simulations are presented in Figure S2 (Supporting Information) for $\lambda = 2$ eV and two different values of the recombination prefactors (k_{r0} and t_{r0}). In that case, an appreciable change of the Fermi level dependence of the diffusion length upon band shift is not observed; hence, we can conclude that only by using an intermediate value of the reorganization energy, which is lower than the two studied values of $E_c - E_{redox}$, the experimental data can be reproduced. In other words, a certain contribution of the well-known Marcus inverted regime is necessary to reproduce the observed behavior.[39] To further clarify this point, the energy distributions for electrons undergoing recombination corresponding to the simulations of Figure 5 are shown in Figure 6 for two different

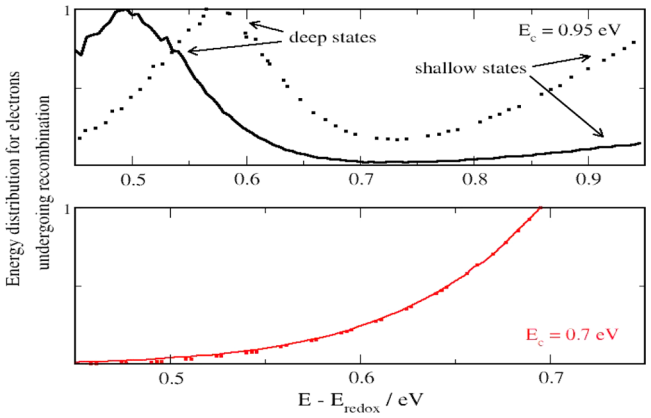

Figure 6. Distribution of energies for electrons undergoing recombination for the two values of the conduction band energy studied in Figure 5. Two Fermi levels are represented for each conduction band position: For $E_c - E_{redox} = 0.95$ eV (top) the cases $E_F - E_{redox} = 0.45$ eV (solid line) and $E_F - E_{redox} = 0.58$ eV (dashed line) are represented. In the same way, for $E_c - E_{redox} = 0.7$ eV (bottom) the cases $E_F - E_{redox} = 0.39$ eV (solid line) and $E_F - E_{redox} = 0.5$ eV (dashed line) are represented. Calculations were carried out using $k_{r0} = 10^{-3}$ arb units and $t_{r0} = 10^7 t_0$.

values of the Fermi level in each case. For $E_c = 0.95$ eV (no additives in the electrolyte), it is observed that the most probable donor energy is located in the vicinity of the quasi-Fermi-level energy and is, therefore, different for each simulated open-circuit voltage. On the other hand, for $E_c = 0.7$ eV (with 2 M Li^+ in the electrolyte), the most probable donor energy is situated in the vicinity of the conduction band position for both cases and does not change with respect to V_{oc}. Therefore, a correspondence is actually observed between the electron diffusion length behavior and the energy distribution function of recombination sites. This observation can be related to the Marcus inverted regime described in Figure 2, where an increasing electron diffusion length is expected when the recombination site is at a higher energy than E_{ox} (the most probable energy of the electron acceptor in solution). In conclusion, the interplay of the Marcus inverted regime and the displacement of the conduction band can correctly explain the change from a V_{oc}-independent to a V_{oc}-dependent diffusion length as a change of the main charge transfer mechanism, from recombination controlled by shallow traps to recombination controlled by deep traps. In fact, when recombination is controlled by shallow traps only, it is the compensation effect between transport and recombination what keeps the diffusion length V_{oc}-independent (see Figure 7 for an illustration of these effects). This is a significant new finding with respect to previous models, where only one type of mechanism (conduction band recombination or deep trap recombination) is considered, and no transport effects are included.

To establish the "degree of nonlinearity" we should estimate the reaction order β with respect to free electron density, as defined by eq 1. As indicated in the previous section, the RWNS method can be utilized to simulate an open-circuit photovoltage decay experiment. The kinetics of the recombination reaction can be numerically extracted by fitting to the expression for the *total* electron density:

$$-\frac{dn}{dt} = kn^{\gamma} \qquad \gamma \neq 1 \tag{13}$$

which can be integrated to give

$$-\int_{n_0}^{n} \frac{dn}{n^{\gamma}} = k\int_0^t dt \Rightarrow n = (At + B)^{1/(1-\gamma)} \tag{14}$$

where A and B are constants. In eqs 13 and 14, the exponent γ is the reaction order with respect to the total electron density. Under quasistatic conditions (internal equilibrium between free and trapped electrons), the total and free electron densities are related to each other. The following relationship can be derived[14,58]

$$\frac{n}{n^0} = \left(\frac{n_c}{n_c^0}\right)^{\alpha} \tag{15}$$

where $\alpha = T/T_0$. Introducing eq 15 into eq 13 and taking into account eq 1, we find

$$\gamma = \frac{\beta}{\alpha} \tag{16}$$

Note that the reaction order with respect to the total electron density (γ) can be larger than one, even when (as it will be discussed below) the recombination rate is sublinear with respect to free electron density ($\beta < 1$).

The result of the fits to the electron density decays between specific Fermi levels in Figure 8 shows that a larger slope of the electron diffusion length with respect to V_{oc} is correlated to a larger degree of nonlinearity of the recombination kinetics. Hence, for the case of $E_c - E_{redox} = 0.7$ eV, where the diffusion length is independent of V_{oc}, as shown in Figure 5, a reaction order of $\beta \sim 0.99$ is obtained. In contrast, for the case of $E_c - E_{redox} = 0.95$ eV, where the diffusion length is dependent on V_{oc} (Figure 5), a value of $\beta \sim 0.78$ is obtained. The results were obtained for a fast recombining system (short diffusion length), hence the short times in which the decay is produced. However, as shown in Figure S1 (Supporting Information), modifying the value of the prefactors in eqs 7 and 8 does change the absolute value of L_n, but not its variation with respect to the Fermi level. Hence, we can conclude that the observed correlation between nonlinear recombination and diffusion length behavior is in

dx.doi.org/10.1021/jp306517g | J. Phys. Chem. C 2012, 116, 22687−22697

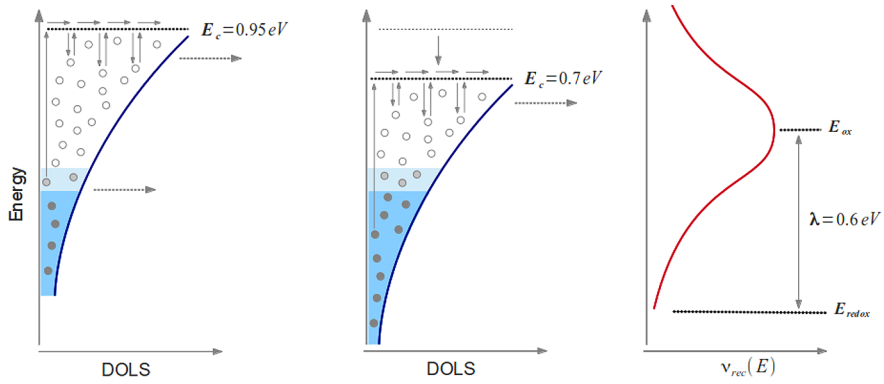

Figure 7. Diagram illustrating the change of recombination behavior with respect to Fermi level variation (symbolized by different shades of blue) when the conduction band is displaced toward lower energies. When the band is at 0.95 eV (left), recombination occurs from both shallow and deep states in a distribution of localized states (DOLS) and the diffusion length increases with increasing Fermi level. This situation corresponds to the top panel in Figure 6. When the band is at 0.70 eV (right), recombination from shallow traps is dominant and the diffusion length is independent of Fermi level. This situation corresponds to bottom panel in Figure 6. In this case, it is the compensation effect between transport and recombination what keeps the diffusion length constant.

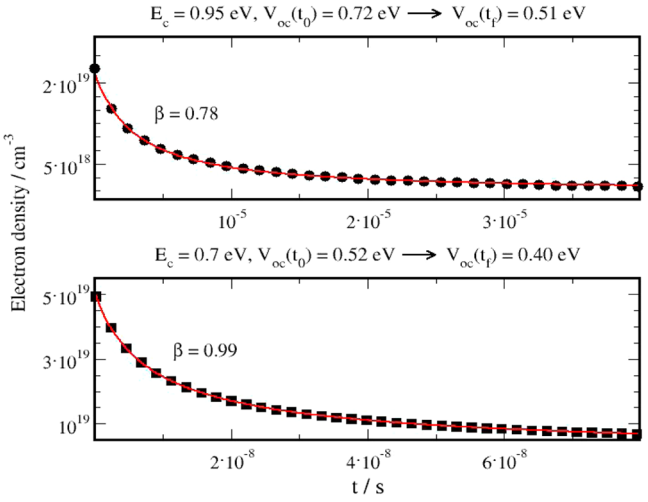

Figure 8. Evolution of the total electron population in a transient RWNS calculation for the same cases as those studied in Figure 5. The solid line represents the result of the fitting to eq 13. Note that results shown correspond to rapid recombination kinetics (short-diffusion length).

agreement with the results of Bisquert and Mora-Seró[18] and Villanueva-Cab et al.[19]

By means of eq 10 the electron lifetime can be extracted from the electron density decays. The results are compared with the electron lifetimes obtained from the steady-state simulations using the averaging procedure in Figure 8. It is found that both methods provide the same results, hence confirming that the behavior of the diffusion length is actually connected to the kinetics of the recombination reaction. It is interesting to note that the behavior of the lifetime is the same as observed in experiments.[20,61] Indeed, the electron lifetime is reduced upon shifting the conduction band to lower energies, meaning that the recombination rate is enhanced. This is an expected characteristic, since when the conduction band is lowered, it gets closer to a fixed Fermi level, which is similar to raising the Fermi level ($E_F - E_{redox}$) toward a fixed conduction band energy. As the recombination rate is increased upon addition of Li^+, the open-circuit voltage of the solar cell at the same illumination intensity is reduced. This suggests that it is kinetics rather than thermodynamics that determines the variation of V_{oc} in a DSC when the semiconductor conduction band is displaced. A similar effect is produced when a redox couple with a different equilibrium potential is used, as is the case for novel redox shuttles, including those based on cobalt complexes.[62−66] On the other hand, Figure 9 shows that the electron lifetime

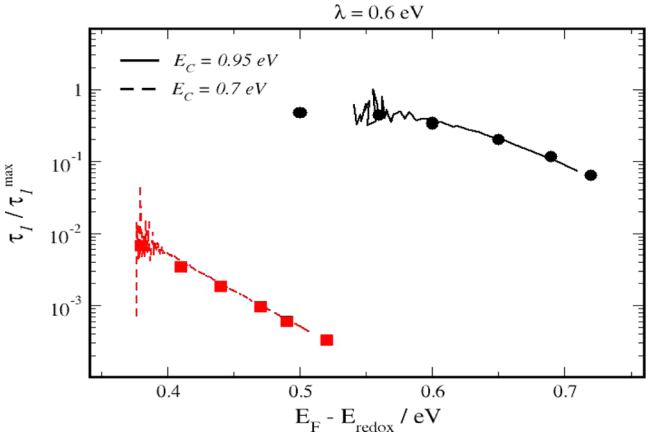

Figure 9. Electron lifetimes for a system defined by λ = 0.6 eV, T_0 = 700 K, T = 300 K, and $E_c - E_{redox}$ = 0.95 (black) and 0.70 eV (red). Symbols stand for results of the steady-state RWNS calculations and lines refer to lifetimes extracted from the transient RWNS calculations and eq 9. Calculations were carried out using $k_{r0} = 10^{-3}$ arb units and $t_{r0} = 10^7 t_0$.

slope for the case of $E_c - E_{redox}$ = 0.7 eV is higher (defined positive) than for the case of $E_c - E_{redox}$ = 0.95 eV. This is consistent with the fact that a compensation effect that maintains the diffusion length constant is accomplished in the first case but not in the second.

CONCLUSIONS

Electron transport and recombination processes in dye-sensitized solar cells are described by means of a random-walk numerical simulation procedure based on the multiple-trapping model, where recombination is explicitly considered using the Marcus−Gerischer theory. This model permits one to relate the nonlinear features of the recombination rate usually found in the experiments with the molecular mechanisms of transport and electron transfer that take place in the

dx.doi.org/10.1021/jp306517g | J. Phys. Chem. C 2012, 116, 22687−22697

nanostructured semiconductor and at the semiconductor–electrolyte interface. Only a hybrid model that takes recombination from shallow traps and from deep traps into account at the same time reproduces all the experimental observations correctly. This work helps one to understand how a nonlinear regime can arise from the relative positions of the Fermi level and the equilibrium redox potential of the electrolyte.

We have observed that nonlinear recombination kinetics can be detected for high values of the reorganization energy. However, only if we consider a driving force for recombination in the Marcus inverted regime, corresponding to a value of the oxidation energy lower than the conduction band position (small or moderate reorganization energy), it is possible to reproduce the experimental observation that a positive band-edge displacement leads to a change in the diffusion length behavior, from being dependent on V_{oc} to becoming independent of V_{oc}. We explain the experimental observation as a consequence of a change in the main recombination mechanism involved in the system, from a shallow traps controlled charge transfer mechanism (constant diffusion length) to a deep traps controlled charge transfer mechanism (diffusion length dependent on V_{oc}). The results are very relevant to understand the performance of new redox shuttles in dye-sensitized solar cells, and further work is being carried out in this respect. Importantly, the model developed here takes into account the Fermi level dependence of the transport kinetics as well, which leads to a constant diffusion length when recombination is controlled by shallow traps. Furthermore, the explicit consideration of transport opens the way to study the system under conditions different from those at open circuit.

■ ASSOCIATED CONTENT

Supporting Information

Additional material as noted in the text. This material is available free of charge via the Internet at http://pubs.acs.org.

■ AUTHOR INFORMATION

Corresponding Author

*E-mail: anta@upo.es.

Notes

The authors declare no competing financial interest.

■ ACKNOWLEDGMENTS

We thank the Ministerio de Ciencia e Innovación of Spain for funding under project HOPE CSD2007-00007 (Consolider-Ingenio 2010) and CTQ2009-10477 and Junta de Andalucía under projects P06-FQM-01869, P07-FQM-02595, and P07-FQM-02600. Funding from CONACyT under Grant number 80002-Y and FOMIX-Yucatán under grant number 170120 is gratefully acknowledged. We also thank Prof. Juan Bisquert for valuable comments and discussions.

■ REFERENCES

(1) Fujishima, A.; Honda, K. *Nature* **1972**, 37–38.
(2) Fujishima; Rao, T. N. *Pure Appl. Chem.* **1998**, *70*, 2177–2187.
(3) Fernandez-Ibanez, P. *J. Colloid Interface Sci.* **2000**, *227*, 510–516.
(4) Leng, W. H.; Barnes, P. R. F.; Juozapavicius, M.; O'Regan, B. C.; Durrant, J. R. *J. Phys. Chem. Lett.* **2010**, *1*, 967–972.
(5) Villarreal, T. L.; Gómez, R.; Neumann-Spallart, M.; Alonso-Vante, N.; Salvador, P. *J. Phys. Chem. B* **2004**, *108*, 15172–15181.
(6) Kamat, P. V. *J. Phys. Chem. Lett.* **2012**, *3*, 663–672.
(7) O'Regan, B.; Gratzel, M. *Nature* **1991**, *353*, 737–740.
(8) Grätzel, M. *Acc. Chem. Res.* **2009**, *42*, 1788–1798.
(9) Graetzel, M. *ChemPhysChem* **2009**, *10*, 290–299.
(10) Katoh, R.; Furube, A.; Barzykin, A. V.; Arakawa, H.; Tachiya, M. *Coord. Chem. Rev.* **2004**, *248*, 1195–1213.
(11) Cai, J.; Satoh, N.; Han, L. *J. Phys. Chem. C* **2011**, *115*, 6033–6039.
(12) Jennings, J. R.; Liu, Y.; Wang, Q. *J. Phys. Chem. C* **2011**, *115*, 15109–15120.
(13) Schlichthörl, G.; Park, N. G.; Frank, A. J. *J. Phys. Chem. B* **1999**, *103*, 782–791.
(14) Lagemaat, J. van de; Frank, A. J. *J. Phys. Chem. B* **2000**, *104*, 4292–4294.
(15) Frank, A. J.; Kopidakis, N.; van de Lagemaat, J. *Coord. Chem. Rev.* **2004**, *248*, 1165–1179.
(16) Fisher, A. C.; Peter, L. M.; Ponomarev, E. A.; Walker, A. B.; Wijayantha, K. G. U. *J. Phys. Chem. B* **2000**, *104*, 949–958.
(17) Bisquert, J.; Fabregat-Santiago, F.; Mora-Seró, I.; Garcia-Belmonte, G.; Giménez, S. *J. Phys. Chem. C* **2009**, *113*, 17278–17290.
(18) Bisquert, J.; Mora-Seró, I. *J. Phys. Chem. Lett.* **2010**, *1*, 450–456.
(19) Villanueva-Cab, J.; Wang, H.; Oskam, G.; Peter, L. M. *J. Phys. Chem. Lett.* **2010**, *1*, 748–751.
(20) Jennings, J. R.; Li, F.; Wang, Q. *J. Phys. Chem. C* **2010**, *114*, 14665–14674.
(21) Bisquert, J. *J. Phys. Chem. B* **2002**, *106*, 325–333.
(22) Fabregat-Santiagoa, F.; Bisquert, J.; Palomares, E.; Haque, S. A.; Durrant, J. R. *J. Appl. Phys.* **2006**, 100.
(23) Wang, Q.; Ito, S.; Gratzel, M.; Fabregat-Santiago, F.; Mora-Sero, I.; Bisquert, J.; Bessho, T.; Imai, H. *J. Phys. Chem. B* **2006**, *110*, 25210–25221.
(24) Gonzalez-Vazquez, J. P.; Anta, J. A.; Bisquert, J. *J. Phys. Chem. C* **2010**, *114*, 8552–8558.
(25) Salvador, P.; Hidalgo, M. G.; Zaban, A.; Bisquert, J. *J. Phys. Chem. B* **2005**, *109*, 15915–15926.
(26) Fabregat-Santiago, F.; Bisquert, J.; Palomares, E.; Otero, L.; Kuang, D. B.; Zakeeruddin, S. M.; Gratzel, M. *J. Phys. Chem. C* **2007**, *111*, 6550–6560.
(27) Guillén, E.; Fernández-Lorenzo, C.; Alcántara, R.; Martín-Calleja, J.; Anta, J. A. *Sol. Energy Mater. Sol. Cells* **2009**, *93*, 1846–1852.
(28) Guillén, E.; Azaceta, E.; Peter, L. M.; Zukal, A.; Tena-Zaera, R.; Anta, J. A. *Energy Environ. Sci.* **2011**, *4*, 3400–3407.
(29) Guillén, E.; Idígoras, J.; Berger, T.; Anta, J. A.; Fernández-Lorenzo, C.; Alcántara, R.; Navas, J.; Martín-Calleja, J. *Phys. Chem. Chem. Phys.* **2011**, *13*, 207.
(30) Barnes, P. R. F.; Anderson, A. Y.; Juozapavicius, M.; Liu, L.; Li, X.; Palomares, E.; Forneli, A.; O'Regan, B. C. *Phys. Chem. Chem. Phys.* **2011**, *13*, 3547–3558.
(31) Zhu, K.; Jang, S.-R.; Frank, A. J. *J. Phys. Chem. Lett.* **2011**, *2*, 1070–1076.
(32) Peter, L. M. *J. Phys. Chem. C* **2007**, *111*, 6601–6612.
(33) Hagfeldt, A.; Boschloo, G.; Sun, L.; Kloo, L.; Pettersson, H. *Chem. Rev.* **2010**, *110*, 6595–6663.
(34) Fabregat-Santiago, F.; Randriamahazaka, H.; Zaban, A.; Garcia-Canadas, J.; Garcia-Belmonte, G.; Bisquert, J. *Phys. Chem. Chem. Phys.* **2006**, *8*, 1827–1833.
(35) Bisquert, J.; Fabregat-Santiago, F.; Mora-Sero, I.; Garcia-Belmonte, G.; Barea, E. M.; Palomares, E. *Inorg. Chim. Acta* **2008**, *361*, 684–698.
(36) Nelson, J. *Phys. Rev. B* **1999**, *59*, 15374–15380.
(37) Kopidakis, N.; Schiff, E. A.; Park, N.-G.; van de Lagemaat, J.; Frank, A. J. *J. Phys. Chem. B* **2000**, *104*, 3930–3936.
(38) Anta, J. A. *Energy Environ. Sci.* **2009**, *2*, 387–392.
(39) Jennings, J. R.; Wang, Q. *J. Phys. Chem. C* **2010**, *114*, 1715–1724.
(40) Bisquert, J.; Zaban, A.; Salvador, P. *J. Phys. Chem. B* **2002**, *106*, 8774–8782.
(41) Anta, J. A.; Mora-Sero, I.; Dittrich, T.; Bisquert, J. *J. Phys. Chem. C* **2007**, *111*, 13997–14000.
(42) Kuciauskas, D.; Freund, M. S.; Gray, H. B.; Winkler, J. R.; Lewis, N. S. *J. Phys. Chem. B* **2001**, *105*, 392–403.

(43) Nakade, S.; Kanzaki, T.; Kubo, W.; Kitamura, T.; Wada, Y.; Yanagida, S. *J. Phys. Chem. B* **2005**, *109*, 3480−3487.
(44) Ondersma, J. W.; Hamann, T. W. *J. Am. Chem. Soc.* **2011**, *133*, 8264−8271.
(45) Ansari-Rad, M.; Abdi, Y.; Arzi, E. *J. Phys. Chem. C* **2012**, *116*, 10867−10872.
(46) Anta, J. A.; Casanueva, F.; Oskam, G. *J. Phys. Chem. B* **2006**, *110*, 5372−5378.
(47) Bisquert, J.; Vikhrenko, V. S. *J. Phys. Chem. B* **2004**, *108*, 2313−2322.
(48) Nelson, J.; Haque, S. A.; Klug, D. R.; Durrant, J. R. *Phys. Rev. B* **2001**, *63*, 6320.
(49) Kopidakis, N.; Benkstein, K. D.; Lagemaat, J.; van de; Frank, A. J. *J. Phys. Chem. B* **2003**, *107*, 11307−11315.
(50) Gonzalez-Vazquez, J. P.; Morales-Flórez, V.; Anta, J. A. *J. Phys. Chem. Lett.* **2012**, 386−393.
(51) Bisquert, J.; Zaban, A.; Greenshtein, M.; Mora-Sero, I. *J. Am. Chem. Soc.* **2004**, *126*, 13550−13559.
(52) Tiedje, T.; Rose, A. *Solid State Commun.* **1981**, *37*, 49−52.
(53) Anta, J. A.; Nelson, J.; Quirke, N. *Phys. Rev. B* **2002**, 65.
(54) Anta, J. A.; Mora-Sero, I.; Dittrich, T.; Bisquert, J. *Phys. Chem. Chem. Phys.* **2008**, *10*, 4478−4485.
(55) Note: The reason for that is that after a jump event the recombination of the electron is recalculated to account for the new energy of the target site. Thus, most of the electrons that may undergo recombination will be those immobile during a time that is long enough to get the shortest recombination time within the list of waiting times.
(56) Hsiao, P.-T.; Teng, H.-S. *J. Taiwan Inst. Chem. Eng.* **2010**, *41*, 676−681.
(57) Barnes, P. R. F.; Anderson, A. Y.; Durrant, J. R.; O'Regan, B. C. *Phys. Chem. Chem. Phys.* **2011**, *13*, 5798−5816.
(58) Anta, J. A.; Idígoras, J.; Guillén, E.; Villanueva-Cab, J.; Mandujano-Ramirez, H. J.; Oskam, G.; Pelleja, L.; Palomares, E. J. *Phys. Chem. Chem. Phys.* **2012**, *14*, 10285−10299.
(59) Villanueva, J.; Oskam, G.; Anta, J. A. *Sol. Energy Mater. Sol. Cells* **2010**, *94*, 45−50.
(60) Ardo, S.; Meyer, G. J. *Chem. Soc. Rev.* **2009**, *38*, 115.
(61) Haque, S. A.; Palomares, E.; Cho, B. M.; Green, A. N. M.; Hirata, N.; Klug, D. R.; Durrant, J. R. *J. Am. Chem. Soc.* **2005**, *127*, 3456−3462.
(62) Ondersma, J. W.; Hamann, T. W. *J. Phys. Chem. C* **2010**, *114*, 638−645.
(63) Nelson, J. J.; Amick, T. J.; Elliott, C. M. *J. Phys. Chem. C* **2008**, *112*, 18255−18263.
(64) DeVries, M. J.; Pellin, M. J.; Hupp, J. T. *Langmuir* **2010**, *26*, 9082−9087.
(65) Bergeron, B. V.; Marton, A.; Oskam, G.; Meyer, G. J. *J Phys Chem B* **2005**, *109*, 937−943.
(66) Oskam; Bergeron, B. V.; Meyer, G. J.; Searson, P. C. *J. Phys. Chem. B* **2001**, *105*, 6867−6873.